

Utilization of Timepix3 Detector for METU-DBL Project Preliminary Test Flux Measurement

B. Bodur^{1,2}, A. Avaroğlu¹, M. S. Aydin¹, M. B. Demirköz^{1,3}, U. Kılıç¹, E. Özipek¹, İ. Şahin¹, A. Tügen¹ and D. Veske¹

¹*Middle East Technical University, Department of Physics*

²*Middle East Technical University, Phys415 Student*

³*Middle East Technical University, Phys415 Supervisor*

June 9, 2017

Abstract

METU Defocusing Beamline (METU-DBL) Project aims to create a facility to perform Single Event Effect radiation tests of electronic equipment, according to ESA ESCC No. 25100 standards. The beamline will be constructed at the end of a 30 MeV accelerator in the Turkish Atomic Energy Authority (TAEK) Sarayköy Nuclear Research and Education Center (SANAEM) Proton Accelerator Facility (PAF). Before testing the electronic equipment at the target area, the flux and uniformity of the 30 MeV proton beam must be measured and their compliance to relevant standards must be verified. Timepix3 Pixel Detector developed by the Medipix Collaboration, is used for this purpose in the METU-DBL. In this study, a method to accurately measure the flux of the proton beam up to a flux of 10^{10} proton/cm²/s, despite clustering and pile-up problems occur at this energy and flux range is proposed. Development of a simulation script for testing the measurement method and result of these tests are also presented. In addition, practical issues such as the development of a control system with LabVIEW, electromechanical structure responsible for movement of the detector through target area, precautions against radiation damage are addressed.

1 Introduction

METU Defocusing Beamline (METU-DBL) [1, 2] Project aims to create a facility to perform Single Event Effect (SEE) radiation tests of electronic equipment. METU-DBL is designed to comply with ESA ESCC No. 25100 standards [3, 4] (Table 1) for SEE tests. For that purpose, a defocusing beamline will be constructed at the end of a 30 MeV accelerator in the Turkish Atomic Energy Agency (TAEK) Sarayköy Nuclear Research and Education Center (SANAEM) Proton Accelerator Facility (PAF).

Measurement of the beam flux and uniformity of the flux in the target area is critical to prove the facility's compliance to ESA ESCC No. 25100 standards. For that purpose, three independent flux measurement systems will be used. First one is a CVD diamond detector, second one is a series of thin scintillating fibers with PIN diode, and last one is the Timepix3 Detector. All three measurement systems will be

Table 1: Requirements of ESA ESCC No. 25100 standards [3]

Parameter	Value
Energy Range	20 MeV - 200 MeV
Flux Range	10^5 proton/cm ² /s to at least 10^8 proton/cm ² /s
Beam Size	15.40 cm x 21.55 cm
Uniformity	$\pm 10\%$

positioned on movable XY stages, hence measurements can be performed over the entire target area. By comparing measured fluxes at different positions, flux uniformity in the target area will also be obtained.

In the following sections, this report details the utilization of Timepix3 Pixel Detector for the flux measurement at the target area of the METU-DBL preliminary test setup.

2 Brief Description of METU-DBL

METU-DBL will consist of quadrupole magnets to enlarge the beam, titanium foils and collimators to reduce the flux in order to obtain the required parameters. A schematic of METU-DBL design can be seen in Figure 1 [4].

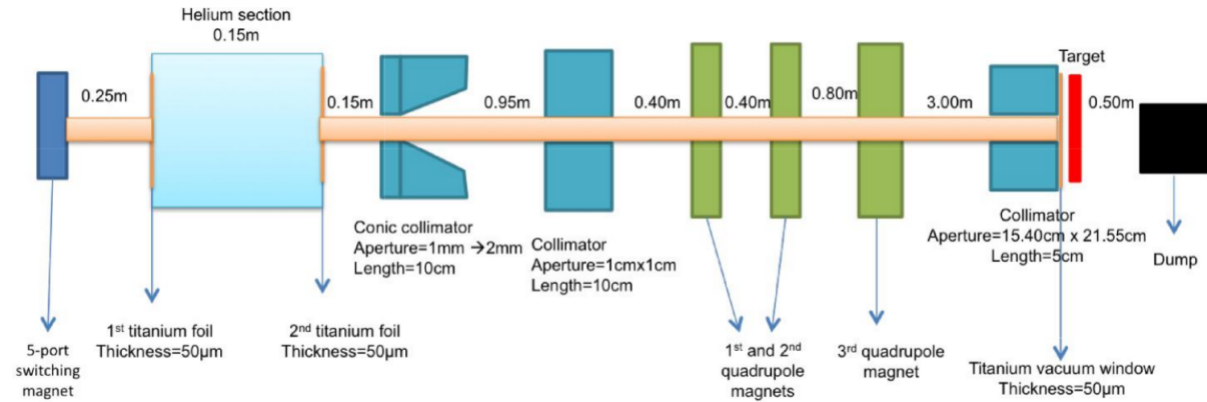


Figure 1: METU-DBL Design Schematic. Collimators and titanium foils reduces flux, three quadrupoles enlarge the beam, a helium section cools the foils [4].

Before the construction of costum designed third quadrupole magnet and arrival of the 5-port switching magnet shown in Figure 1 [4], a preliminary test beamline will be constructed. The beam optics design schematic and mechanical drawing of this beamline can be seen in Figures 2 and 3 [4].

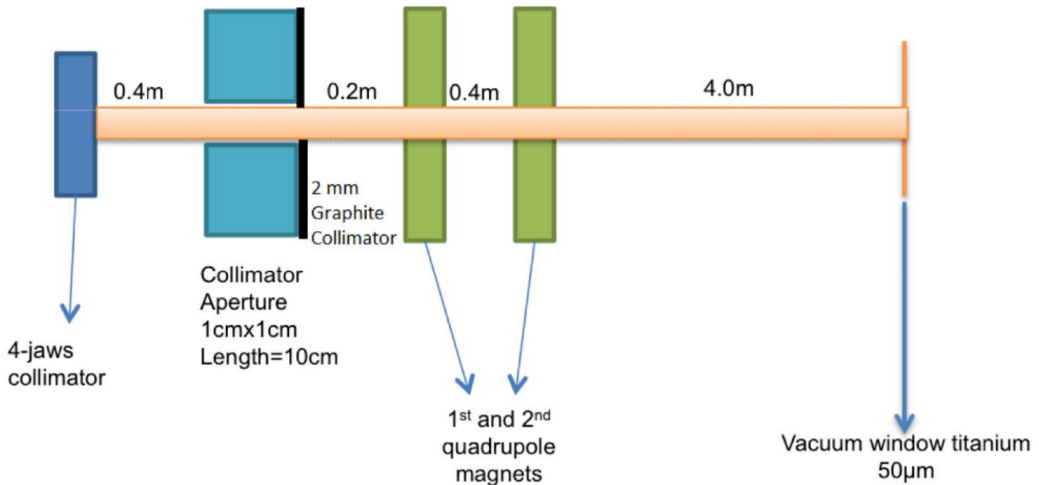


Figure 2: METU-DBL Preliminary Test Design Schematic. The design includes two commercial quadrupole magnets in contrast to three quadrupoles in the final design of the METU-DBL [4].

With the preliminary test configuration in the Figure 2, the position and energy distributions of the protons at the target area would be as in Figure 4 [4]. The results are obtained by using G4beamline

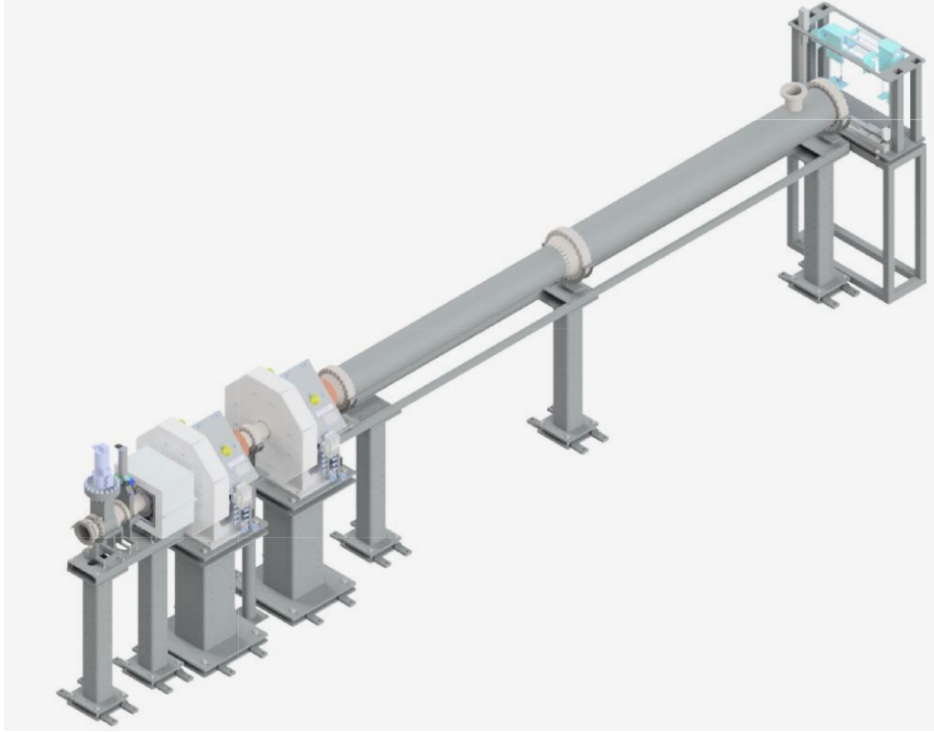


Figure 3: METU-DBL Preliminary Test Setup Mechanical Drawing. Components of beam optics, beam pipes, support tables, and all connectors are drawn on scale [4].

simulation software. The 4 cm x 6 cm uniform flux area seen in Figure 4a, is smaller than the area required by the standards, but with the addition of the last quadrupole, final METU-DBL will satisfy the standards.

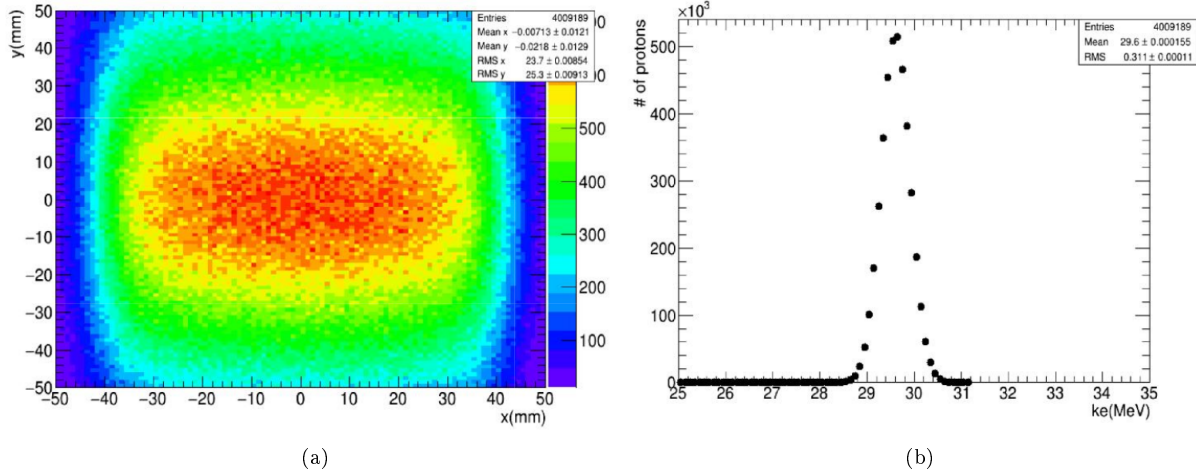


Figure 4: Expected Position (a) and Energy (b) Distribution of the Protons at the Target Area in the METU-DBL Preliminary Test Setup. The results are from G4beamline simulation of the beamline, with 10^8 initial particles. In (a) there is a 4 cm x 6 cm uniform (within $\pm 10\%$) area with 1.4×10^9 protons/cm 2 /s flux [4].

METU-DBL preliminary tests are expected to be performed in June 2017. A recent photograph of the beamline during the mechanical setup were shown in 5.



Figure 5: The current situation of the mechanical setup of preliminary test configuration of METU-DBL.

3 Mechanical Setup

In Figure 2, a thin vacuum window separating the vacuum in the beamline from the air in the test room can be seen. After that point until the detectors (or test card), particles travel through air, and in order to minimize the distortion of uniformity and the energy loss this distance must be minimized. Figure 6 shows the mechanical design of the table in the target area that holds the detectors and the test card. With this configuration all test cards and detectors were placed within 7 cm from the vacuum window. In the final version of METU-DBL, this distance will be shortened to 5 cm.

The XY stage that will carry the Timepix3 and enable measuring the flux in multiple positions can be seen in Figure 7. This stage will be positioned on the target table seen in Figure 6 and controlled via LabVIEW from the control computer.

4 Measurement with Timepix3 and Data Analysis

Timepix3 is a versatile silicon pixel detector with various acquisition modes. It can measure time of arrival (ToA) of particles to individual pixels with sub-nanosecond resolution, time that signal spends time over a threshold level (ToT), or simply count the number of particles that hit pixels in the given acquisition time [5, 6]. This versatility results in its use in various areas from beam profiling to X-ray imaging. It can be used in data driven mode, where an event at a pixel is read immediately, allowing the pixel to be available for measurement after the readout; or it can be used in a frame based mode, where each pixel is read at the end of the frame. In this mode, a pixel is not able to record a second measurement within the same frame, since its data registers will already be occupied.

Despite the versatility of Timepix3, there are a number of problems encountered for its use with a 30 MeV proton beam where the flux that can reach 10^{10} protons/cm²/s. First problem is due to the high dE/dx of 30 MeV protons in the pixels. In 300 μ m thick pixels, 30 MeV protons will lose, on average 1 MeV of energy (through Bethe-Bloch equation [7]), which will result in 300000 electron-hole pairs (electron yield of silicon is 1 per 3.2 eV [7]). The diffusion of these electrons to neighbouring pixels, ionization through delta-rays, or simply the passage of a proton through multiple pixels cause signals created in a cluster of pixels rather than just one. In Figure 8, real clusters due to alpha particles from an Am241

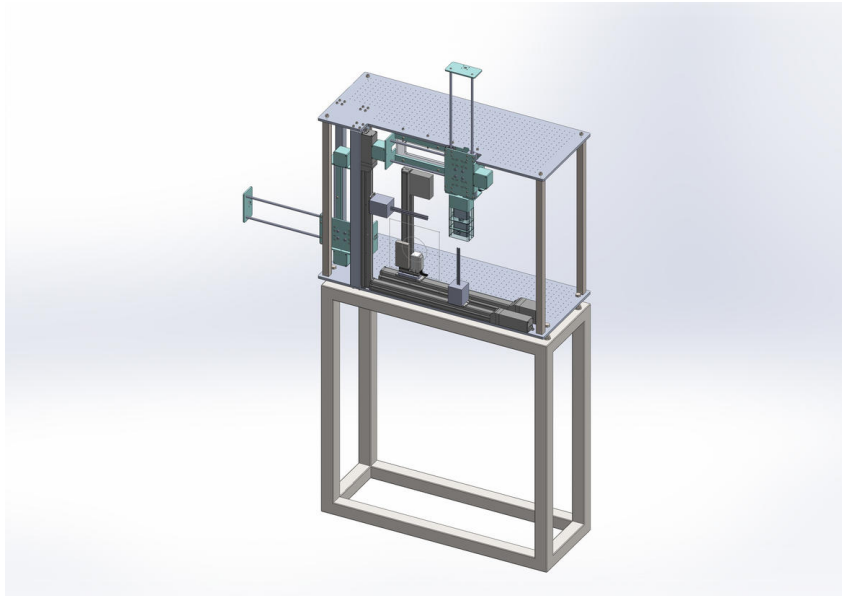


Figure 6: METU-DBL Preliminary Test Setup Target Area Detector and Test Card Holder and Table. Test card, diamond detector, Timepix3 and scintillators. All test and measurement systems will each be on movable trays and placed within 7 cm from the vacuum window.

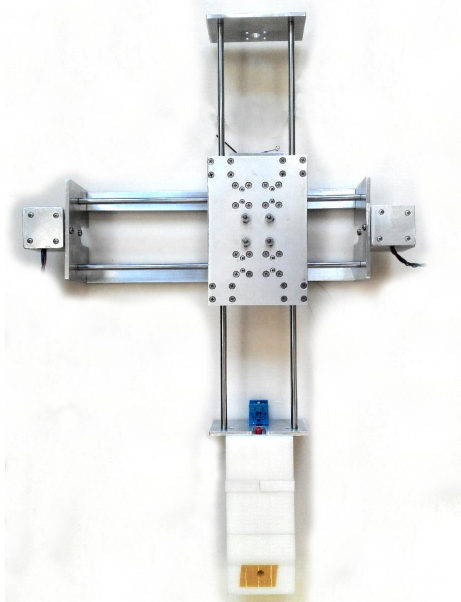


Figure 7: XY stage made from 6082 grade Aluminum. Here, the diamond detector, which is protected by polyethylene and aluminum shielding is attached to the XY stage. Similarly, Timepix3 will be attached to an XY stage of a similar design.

source are shown. Thus, simply counting the number of events through a definite period of time will give inaccurate results. A solution is to use ToA information, so that neighbouring pixels with very close arrival times can be identified, and clusters can be reduced to one particle events.

Another, major problem is the relatively high flux value causing pile-up of pulses, which results in missing a number of particles. To counter this problem effectively, high thresholds and short pulse lengths (high I_{Krum} parameter) [5] must be utilized.

0	0	1502	1503	0	0	0	0	0
0	0	0	1502	1502	0	0	0	0
0	0	0	1503	0	0	0	0	0
304	0	0	0	0	0	0	0	0
0	304	0	0	0	0	0	0	0
0	0	0	0	0	0	0	15068	15068
0	0	0	0	5478	5478	0	15068	15069
0	0	0	0	5477	5477	5477	15067	15068
0	0	0	0	5478	0	0	0	0

Figure 8: Clustering Caused by Alpha Particles From an Am241 Source. In pixels ToA data in terms of 25 ns clock cycles can be seen. Notice that neighbour pixels have very close (or same) ToA. The acquisition time was 1 second, threshold is at 85 keV and I_{Krum} parameter was 255. Each highlighted cluster should be counted as a single alpha particle.

Even at 10^8 protons/cm²/s, a 55 μ m x 55 μ m pixel of Timepix3 [5] will be exposed to 3kHit/s event rate. However, maximum data driven readout speed per pixel (when all pixels are used and uniform distribution of events are assumed) when ToA is enabled, is 1.2 kHit/s. Therefore, instead of using data driven mode, frame based acquisition with low acquisition time (1-10 us) was preferred.

In frame based mode, ToA and ToT information can be recorded at the same time, however ToA and hit count information cannot be recorded simultaneously. ToA information is needed for declustering, therefore flux cannot be measured with the conventional technique, where number of particles coming in a specific time in a specific area are measured. Instead, a method (explained in Section 4.1) based only on ToA information was developed for the proton flux measurement at the target area of METU-DBL and METU-DBL preliminary test set up.

4.1 ToA Method for Declustering and Flux Measurement

First step for flux measurement is declustering with the use of ToA information. The declustering algorithm checks the pixels starting from the one with the smallest ToA. Then it checks first, second and third order neighbouring pixels ¹ for close ToA's ² and marks them as completed along with the original pixel. This process is continued for all ToA's and until all pixels with events marked as complete. This way, correct number of particle events can be found.

The second step is to find out the effective measurement time. As mentioned earlier, a pixel will not record a second hit in frame based mode. Therefore effective measurement time is actually the ToA of the first hit to a pixel. If there is no event during the entire shutter time at a pixel, then measurement time is recorded as shutter time but no contribution to proton events comes from that pixel. These processes are shown in the timing diagram in Figure 9. Pixels 1, 2 and 3 show that effective measurement time is ToA of the first event, and is independent of the number of events (with or without pile-up) that happened after the first hit. Notice that in Pixel 2 and Pixel 3, there are actually more than event in a frame. There is no way to record these events, but this is not a problem since these events did not occur during the effective measurement time.

If a pixel registers an event, but the analysis algorithm decides that signal is due to a hit on a neighbouring pixel, then the measurement time of that pixel is recorded as ToA of the event, but no contribution to proton events come from that pixel.

¹See Figure 10a for definition of neighbouring pixels and degrees.

²Closeness is defined with a user entered parameter and might be different for different neighbouring degrees.

A particle can create a cluster of events at some pixels before the shutter time, but due to the length of the signal they might be recorded in the first clock cycle after the shutter starts. This case is shown in Pixel 4 of Figure 9. In such a case there is no way of knowing when actually these events happened, and therefore all events with ToA equal to or less than first clock cycle, and their clusters were removed from the dataset.

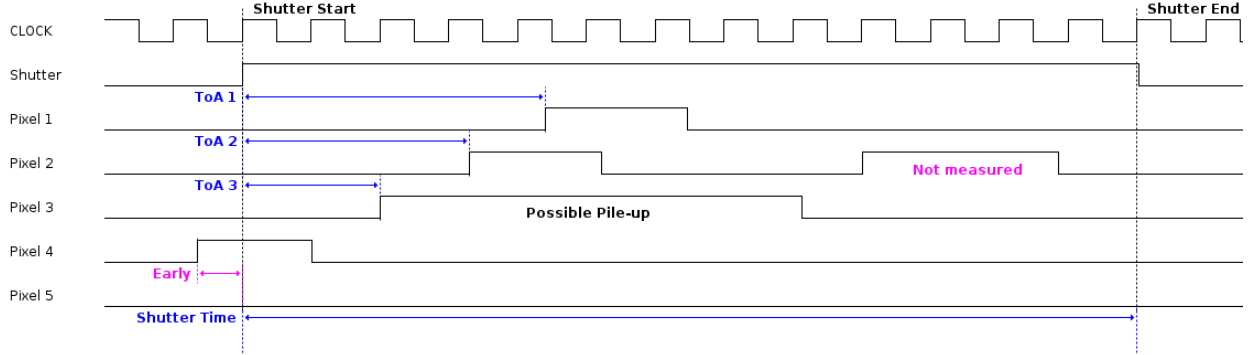


Figure 9: Measurement Method Illustrated on a Timing Diagram. The signals with blue are counted, the signal with label “not measured” in pixel 2 is not measured in frame based ToA + ToT mode, the signal with label “early” in pixel 4 is counted in the first clock cycle of the shutter but discarded during the analysis, the signal with label “possible pile-up” in pixel 3 is counted as a single hit. Missed hits are not a problem in this measurement method since we are not interested in the measurement period after the arrival of the first particle.

$$Flux = \frac{1(Pixel1) + 1(Pixel2) + 1(Pixel3) + 0(Pixel5)}{PixelArea \times (ToA1 + ToA2 + ToA3 + ShutterTime)} \quad (1)$$

For the five pixels shown in Figure 9, the total flux can be calculated by dividing the total number of counts to the total effective measurement time³ as in the Equation 1.

4.2 Simulation with High Fluxes

Before the utilization of the developed method, it should be tested at flux levels of the METU-DBL. Since the response of the detector could only be tested with a low activity Am241 source, a simulation capable of generating the detector’s response to high fluxes was designed in MATLAB.

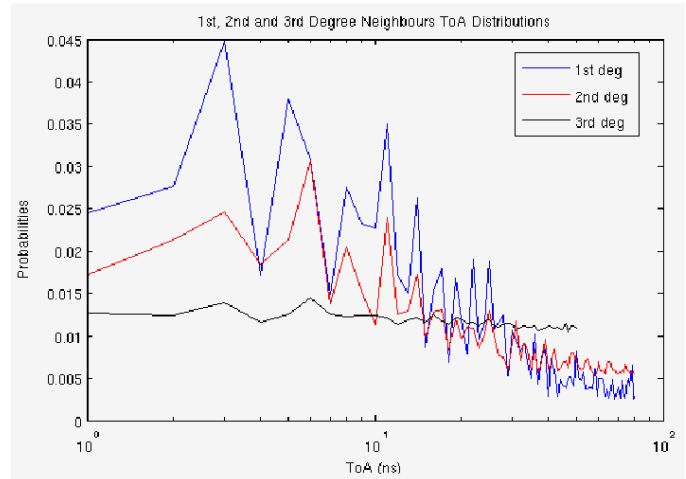
For that purpose, 2500 frames of 400 μ s long measurement of an Am241 source at various distances (from 4 to 21 mm) were performed. Low acquisition time ensures that clusters are easily separable. Then, neighbouring degrees to a pixel were defined as in Figure 10a, so that clustered pixels at different distances to the original pixel can be analyzed separately. Then, the number of extra signals at different neighbouring degrees for every pixel (called occupancy of that neighbouring level) were recorded, and the expected number of occupancies at different neighbouring degrees were extracted as shown in Table 2. From the table, it is clear that occupancy decreases as neighbouring degree increases as expected. Lastly, difference of center and neighbouring ToA’s for each degree were recorded and ToA difference distributions were obtained as in Figure 10b.

A MATLAB script generating Poisson distributed hits in time, according to a uniform flux in position was implemented. For each hit, clusters were generated according to previously obtained real occupancy and ToA distributions. In order to replicate a real measurement, simulations involve a time larger than the intended shutter time, so that a non-ideal situations such as arrival of particle just before shutter starts (as in Pixel 4 in the Figure 9) can arise.

³Or by dividing average counts per pixel to the average measurement time, which leads to the same equation.

3	3	3	3	3	3	3	3
3	2	2	2	2	2	2	3
3	2	1	1	1	2	3	
3	2	1	0	1	2	3	
3	2	1	1	1	2	3	
3	2	2	2	2	2	3	
3	3	3	3	3	3	3	3

(a)



(b)

Figure 10: Definition of Neighbouring Degrees (a) and Distribution of Difference From the Center ToA for Each Neighbouring Degree (b). Pixel numbered with 0, is the pixel with the lowest ToA in the cluster. Measurements for obtaining these distributions were again performed with Am241 source.

Table 2: Expected Occupancy of the Alpha Particles From an Am241 Source. It is clear that as distance from the pixel with the first hit increases, expected occupancy decreases. Measurements were performed in various source-detector distances from 4 to 21 mm.

Neighbouring Degree	Expected Occupancy
1	0.888
2	0.402
3	0.009

The simulation results were written to “pixel multi frame (.pmf)” files same way as the original measurements were recorded, and feeded to the analysis code. The obtained flux for these simulated data are given in the Table 3.

Table 3: Simulated and Measured Fluxes, and Their Percent Differences. Up to $2.00 \times 10^{10} \text{ p/cm}^2/\text{s}$ flux, the percent difference is equal to or less than 1%. After that flux, declustering algorithm starts to count two closely separated (both in time and position) particles as one. The acquisition time for these simulations and measurements were 2500 ns, same as the planned acquisition time in real measurements.

Simulated Flux $\text{p/cm}^2/\text{s}$	Measured Flux $\text{p/cm}^2/\text{s}$	Percent Difference %
1.00×10^7	1.00×10^7	0.00
1.00×10^8	1.00×10^8	0.00
1.50×10^9	1.49×10^9	-0.67
3.00×10^9	3.03×10^9	1.00
5.00×10^9	5.05×10^9	1.00
7.00×10^9	7.04×10^9	0.57
1.00×10^{10}	9.96×10^9	-0.40
2.00×10^{10}	1.90×10^{10}	-5.00
4.00×10^{10}	3.43×10^{10}	-14.3

From Table 3, it is possible to see that up to 2.00×10^{10} p/cm²/s, discrepancy from the original flux is less than %1. For fluxes lower than 1.00×10^8 p/cm²/s, there is no discrepancy. This is expected since declustering is simpler at lower fluxes and earlier hits than shutter start time are much less common.

Clustering data is extracted for 5.5 MeV alpha particles from the Am241. This clustering effect is expected to be less for protons, because of the lower energy loss and divergence of protons.

4.3 Uncertainty Considerations

There are two sources of errors in this measurement technique. One is the statistical uncertainty due to the Poisson distribution of the hits, and the second is the uncertainty due to the quantization of timing. In addition, there is 0.4 mm uncertainty in position of the detector due to the precision of the XY stage.

When fast ToA (fToA) [5] is utilized in addition to the regular ToA, the precision of ToA measurement becomes 1.56 ns. During the analysis all ToA values are rounded to multiples of 1 ns, for a faster analysis⁴ and hence the timing precision decreases to 2 ns.

Statistical error of Poisson distributed hits, are simply the square root of the number of hits. This statistical error is in the order of 0.1 % if the total number of counts over the whole detector is used, in the flux range we are interested, with a measurement of 10 frames each having 2500 ns acquisition time. However, the pixel matrix is 1.4 cm x 1.4 cm, and for validation of uniformity higher positional resolution might be required. In that case, the analysis code can divide the whole detector into 16 x 16 equal pixel groups, increasing statistical error by 16 times with the same measurement settings. With this division, position resolution of the flux is in the same order as the positional error due to the precision of XY stage.

$$\Delta Flux = \sqrt{\left(\frac{\Delta Hit}{Area \times Time}\right)^2 + \left(\frac{-Hit}{Area \times Time^2}\right)^2 (Area \times \Delta Time)^2} \quad (2)$$

In order to find the uncertainty in the flux measurement, two error sources might be combined as in Equation 2. The number of 2500 ns long frames and pixel groups will be arranged to make uncertainty in the flux less than 1%.

5 Readout and Control of Timepix3

For readout of the Timepix3 chip, AdvaDAQ card and Pixet Software [8] will be used. The measurements will be performed using the python scripting functionality of the Pixet Software. During measurements, Pixet Software will run on an SBC (Single Board Computer) connected to AdvaDAQ in the test room. A simple socket server will be built on the SBC using Python 2.7. The main control computer of METU-DBL (running LabVIEW), will communicate with this computer through Ethernet.

5.1 Development of the Control System of Timepix3 via LabVIEW

The user interface and control system developed on the LabVIEW should be able to:

- Request a measurement and get the raw measurement file from Timepix3.
- Check temperature and other critical functions of Timepix3.
- Control the XY stage, get the XY stage position.
- Analyze the raw data to obtain flux by utilizing the previously described algorithm.
- Correlate position and flux information.
- Display performed measurements in a graph in real time.

⁴A short analysis time is required since visualisation of flux and uniformity in the target area should be immediately after the measurement

- Record current results to a log file in real time.
- Take scan range and other parameters user input.
- Provide uniformity and uncertainty information about a particular user selected area.
- Quick and efficient to reduce radiation exposure of the detector.

The connections of Timepix3 and AdvaDAQ to the SBC, in addition to the screens of SBC and control computer can be seen in Figure 11.

When the program runs, it will first ask the user the range to scan. This screen can be seen in

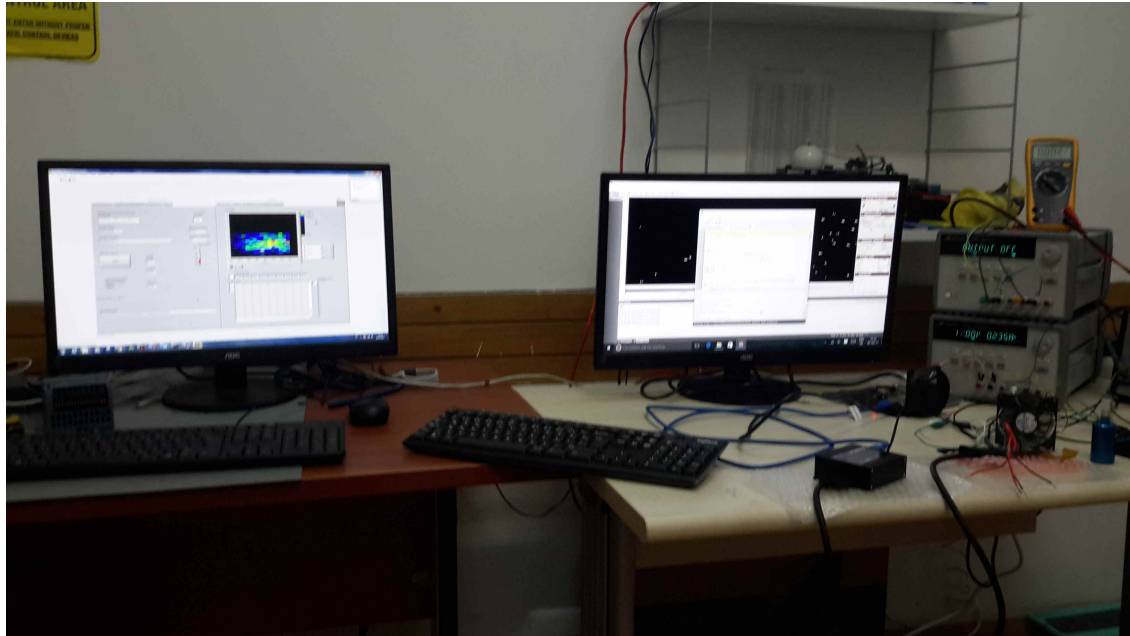


Figure 11: The readout system. SBC is on the right running Pixet and waiting measurement command from the control computer. On the right, the control computer running a LabVIEW based user interface.

Figure 12. In addition this screen includes controls about, row and column division of the Timepix3 and other measurement parameters. When these parameters were entered by the user, they will be adjusted slightly by the control program based on the limits of the scan area and detector size. After the approval of the user, an automatic scanning starts. The program first moves the XY stage to the next measurement position, then requests a measurement from Timepix3, and gives the measurement to the analysis code mentioned in the previous chapters. After the analysis, the data is placed to the appropriate position in a matrix, graphed and recorded to a file. This process is repeated until all the positions in the scan range were covered.

After the completion of the scan, the program prompts user for an analysis area within the scan range, as in Figure 13. The uniformity of the flux within this area, and other results were displayed on this screen.

An example plot of a real measurement were given in Figure 14. Overall, a LabVIEW based control program with the above properties was designed and implemented.

6 Radiation Considerations

Since the beam area is large, Timepix3's peripheral parts, in addition to its sensitive area, will unavoidably be exposed to beam. Several measures are taken to operate Timepix3 in the beam with minimal

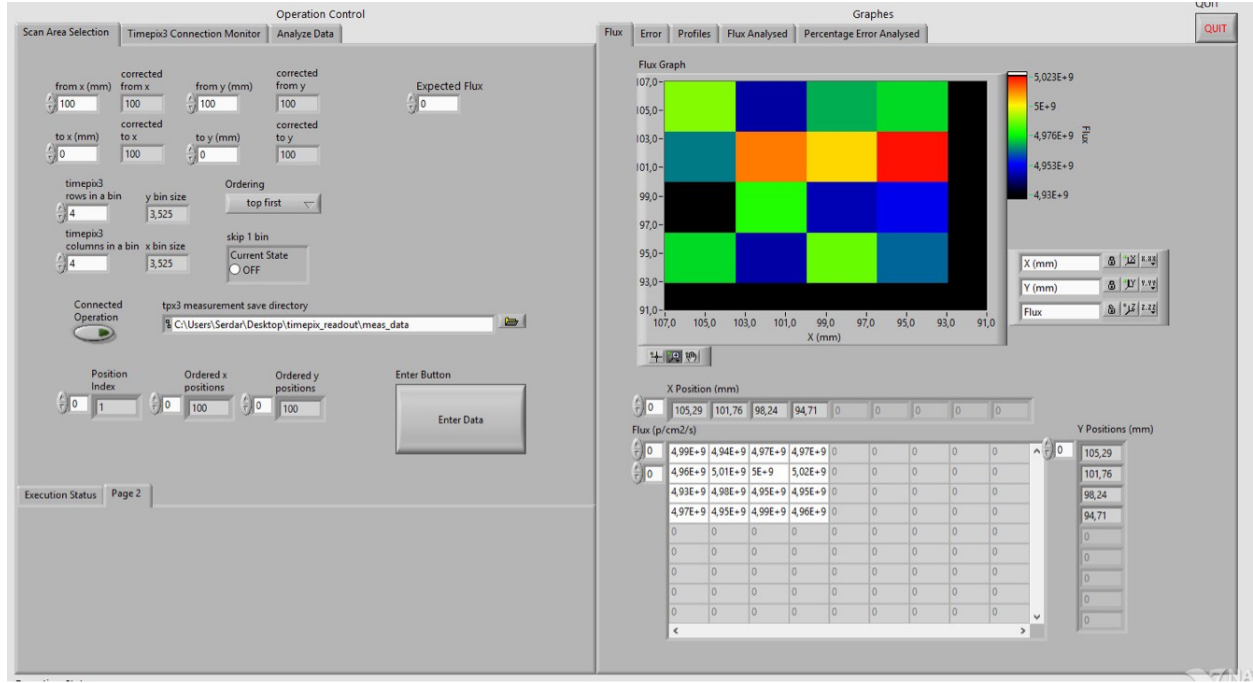


Figure 12: The scan area input of the user interface. The values of the measurements up to now were visualized as a table and as a graph in the right hand side of the user interface.

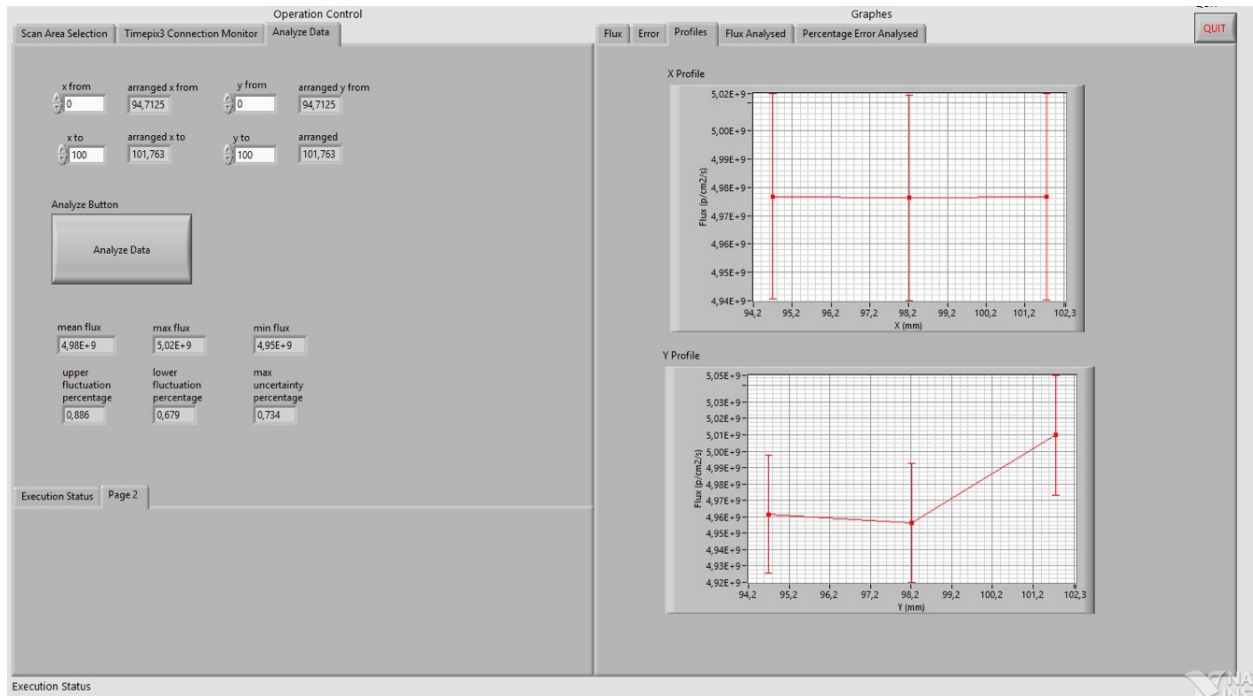


Figure 13: The analysis area input of the user interface. Below the analyze command, the uniformity of the proton flux at the selected area is calculated and displayed. On the right side one dimensional profiles of the beam are displayed.

damage. First of all, Timepix3 and AdvaDAQ will be connected with VHDCI cables [9], so that AdvaDAQ can be positioned outside the beam.

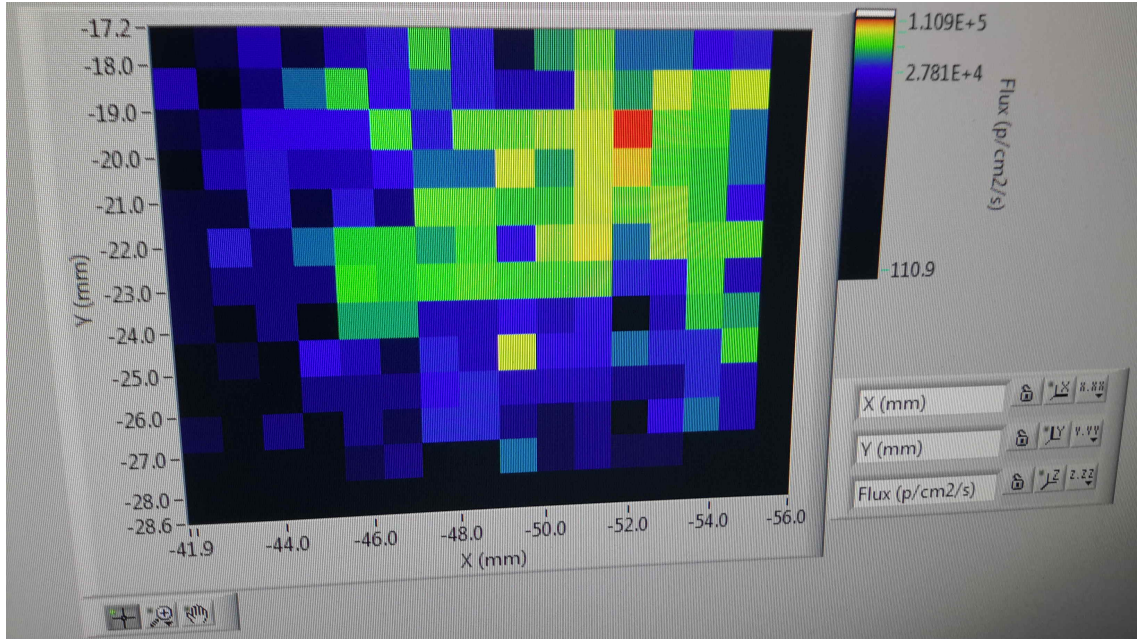


Figure 14: The distribution of alpha particle flux from an 370 kBq Am241 source on the detector.

6.1 Obtaining The Male-Female VHDCI Cable

Because AdvaDAQ was built as a direct connection to Timepix3, it has a male connector fitting the female connector of the Timepix3 chip. However, normally chips or interfaces with VHDCI connectors possess female connectors and only male-male cables are manufactured serially to connect these interfaces. Therefore, finding the required cable was a considerable problem, solved only by obtaining it from the Medipix Collaboration, which gives mass production orders to private companies for such a rare cable in order to be used by similar applications to ours. The acquired male to female 68 way VHDCI cable was shown in Figure 15.



Figure 15: 68 way male-female VHDCI cable, connecting Timepix3 and AdvaDAQ

During the search, two attempts were made to replicate such a cable, however due to the incompatibility of our PCBs and cables with the required LVDS (Low Voltage Differential Signaling) Standards employed for the communication between Timepix3 and AdvaDAQ, these attempts were failed. The voltage signal of a data pin, when Timepix3 were connected to AdvaDAQ directly and with a cable of our own design were shown respectively in Figures 16 and 17.



Figure 16: Voltage Signal on Timepix3 Data Input-Output Pins when Timepix3 is connected to the AdvaDAQ directly. The signal was measured by measuring voltages of both plus and minus connection with respect to ground. The signals in the background represent the individual voltage signals, while the largest signal represent the voltage difference between the terminals, which is the actual signal used to communicate between Timepix and AdvaDAQ. The signal is obtained via a Teledyne Lecroy Waverunner 8000 model oscilloscope.

Approximately 100 mV voltage peak voltage difference between Figures 16 and 17 was because of our failure to comply with the LVDS standards [10]. The LVDS protocol relies on carrying the signal differentially on two cables, thus taking advantage of noise cancellation, since both cables will be subject to the same noise with respect to their common ground, if cables could be arranged to have the same route. On the other hand, since both cables carry a dynamic signal any phase difference between them (due to length difference) may cause reductions in the differential signal strength. Because of routing limitations, all signal pairs could not be moved through to same path (they could not even be arranged in same length) in our design, which resulted with the voltage drop between the Figures 16 and 17.

6.2 Other Precautions

In addition, both AdvaDAQ and Timepix3 (apart from the pixels) will be protected with a 1.2 cm thick shielding which will be composed of aluminum (grade 6082), lead and polyethylene [11, 12]. The shield thickness is designed to be enough to stop 30 MeV protons⁵. In addition FLUKA simulations to calculate the dose Timepix3 will receive were performed [11]. According to these simulations, at 10^9 proton/cm²/s flux, peripherals of Timepix3 will be exposed to 80 rad in 5 minutes [11] of operation in the beam.

Finally, voltage regulators which are not radiation hard, on the chip are planned to be bypassed and chip will be powered externally as Dr. Lukas Tlustos [9] suggested, so that lifetime of the regulators in radiation, will not limit the lifetime of the chip.

⁵ projected range in Al is smaller than 5 mm



Figure 17: Voltage Signal on Timepix3 Data Input-Output Pins when Timepix3 is connected to the AdvaDAQ with a cable of our own design. The signal was measured by measuring voltages of both plus and minus connection with respect to ground. The signals in the background represent the individual voltage signals, while the largest signal represent the voltage difference between the terminals, which is the actual signal used to communicate between Timepix and AdvaDAQ. The signal is obtained via a Teledyne Lecroy Waverunner 8000 model oscilloscope. Notice the decrease of signal when compared to Figure 16.

7 Conclusion

In this report, the utilization of the Timepix3 Pixel Detector for obtaining proton flux distribution in the METU-DBL target area is described in detail. In addition to the analysis method, practical issues such as control and readout of the detector, electromechanical structure responsible for movement of the detector through target area, precautions against radiation damage are also mentioned.

The setup for preliminary test of METU-DBL is currently finalizing and preliminary tests will start within this month. Timepix3 detector and its XY stages can now be fully controlled with a LabVIEW based control system. After the mechanical mounting of Timepix3 on the XY stages, and powering it electrically the measurement system will be operational for the preliminary tests.

8 Acknowledgment

Authors thank to Medipix Collaboration, specifically Prof. Dr. Lawrence Pinsky of University of Houston and Dr. Lukas Tlustos of CERN. Without their kind help, this study and report would not be possible. In addition, authors want to thank to METU ESRAP group members for their support and help.

References

- [1] B. Demirköz, A. Gencer, D. Kızılıören, and R. Apsimon, “Proposal for an irradiation facility at the taek sanaem proton accelerator facility,” *Nuclear Instruments and Methods in Physics Research Section A: Accelerators, Spectrometers, Detectors and Associated Equipment*, vol. 730, pp. 232–234, 2013.
- [2] A. Gencer, B. Demirköz, I. Efthymiopoulos, and M. Yiğitoğlu, “Defocusing beam line design for an irradiation facility at the TAEA SANAEM proton accelerator facility,” *Nuclear Instruments*

and Methods in Physics Research Section A: Accelerators, Spectrometers, Detectors and Associated Equipment, vol. 824, pp. 202–203, 2016.

- [3] ESCC and ESA, *Single Event Effect Test Methods and Guidelines*, 2014.
- [4] M. Yiğitoğlu, *Radiation Environment Predictions for the IMECE Satellite and G4beamline Simulations For The METU-DBL Project*. PhD thesis, METU, February 2017.
- [5] X. Llopert and T. Poikela, *Timepix3 Manual v1.9*. CERN, 2014.
- [6] M. Schut, *Characterisation of the Timepix3 chip using a gaseous detector*. PhD thesis, University of Amsterdam, February 2015.
- [7] C. Grupen and B. Shwartz, *Particle Detectors*. Cambridge, UK: Cambridge University Press, 2011.
- [8] ADVACAM, *PixetPro User's Manual*.
- [9] L. Tlustos. personal communication.
- [10] Altera Corporation, *Board Design Guidelines for LVDS Systems*, 2010.
- [11] P. Uslu. personal communication.
- [12] S. Uzun Duran. personal communication.